International Journal of Materials Chemistry and Physics
Vol. 4, No. 1, 2018, pp. 1-12
http://www.aiscience.org/journal/ijmcp
ISSN: 2471-9609 (Print); ISSN: 2471-9617 (Online)

Removal of Industrial Arsenic (III) and Mercury (II) Pollutant from Wastewater by Fish Scales Waste Materials

Morlu Stevens*, Bareki Batlokwa

Department of Chemical and Forensic Sciences, Botswana International University of Science and Technology, Palapye, Republic of Botswana

Abstract

In this work, pulverized vinegar treated fish scales waste was used as a cheap green adsorbent for the simultaneous removal of high levels of arsenic (III) and mercury (II) from industrial wastewater. After mechanical pulverization and sieving of the collected fish scale waste, it was morphologically evaluated employing SEM. The investigation revealed spherical, rough surface particles with sizes of ≤63 µm. The prepared powder was treated with vinegar to functionalize the surfaces of the particles. Optimal adsorption capability of the treated powder was evaluated by investigating the effects of treated material dosage, pH, initial concentration of the selected ions and the contact time via subjecting the treated material to batch adsorption experiments modeled using Minitab 14 software. The investigation results indicated that, the adsorption of the selected metal ions by the vinegar treated fish scale waste was treated material dosage, pH, initial selected ions concentration and contact time dependent. Langmuir isotherm model was best fitted for the adsorption mechanism of the treated material. The obtained optimal capacity of the treated materials per gram was: 36 mg/g and 34 mg/g for arsenic (III) and mercury (II) respectively. It was also shown that adsorption of the selected ions on the treated material was endothermic, spontaneous and in an orderly fashion.

Keywords

Fish Scales Waste-Remains, Mercury, Arsenic, Wastewater and Adsorption

Received: April 1, 2018 / Accepted: May 21, 2018 / Published online: June 14, 2018

1. Introductions

The environmental challenges as a result of globalization and rapid industrialization are increasingly becoming a nuisance for human beings [1]. Therefore, robust and effective methods are needed particularly for water treatment. The presence of heavy metals in wastewater and industrial effluent is a major concern of environmental pollution. Heavy metals are generally referred to those metal ions whose density exceeds 5 g/cm^3. In recent years, there has been an increasing environmental and worldwide public health concern associated with environmental contamination by these metals [2, 3]. Moreover, human exposure has risen intensely as a result of the persistent exponential use in several industrial, agricultural, domestic and technological applications [4]. They are extremely water soluble, well-known toxins (especially in high concentrations) and carcinogenic agents [5]. Some heavy metals are considered 'troublesome and extremely dangerous' because of their characteristics and pathologies, for example mercury. With the assumption that heaviness and toxicity are inter-related, heavy metals also include metalloids, such as arsenic, that are able to induce toxicity at low levels of exposure [6]. Mercury (II) and Arsenic (III) have been purposely targeted for removal due to their co-existence, toxic characteristic and pathogenic nature [7]. Also, in Palapye, Botswana being an

* Corresponding author
E-mail address: morlu.stevens@studentmail.biust.ac.bw (M. Stevens)

industrial village, and the initial point of implementation of the research findings, these two toxic ions were selected as it is believed that the nature of industrialization may have led to potentially high levels of these ions in the region [8].

Mercury and arsenic, occur in both organic and inorganic forms in the environment, and are toxic elements for human health that persist and cycle in the environment as a result of natural and anthropogenic activities. Anthropogenic sources are mostly transportation [9], mining, smelting, refining, waste incineration, and fossil fuel combustion [10]. Mercury and arsenic pollution from these sources are inevitable, for example, transportation and fossil fuel combustion, hence it is paramount that robust and effective removal methods be introduced to help control the level of heavy metals in the environment. For instance, fossil fuels combusted largely during industrialization and urbanization, contain various heavy metals, such as lead, zinc, mercury and arsenic. It has been reported that gasoline contains 0.2 – 3.3 ng/g mercury and 30–120 ng/g arsenic [11]. Emissions due to transportation and industrial activities can contribute to mercury and arsenic pollution, especially via combustion in the atmosphere [12]. The pollutants are then deposited onto the earth forming dust or directly enter water and soil, affecting their quality via dry and wet deposition processes. Wastewater is the most affected by mercury and arsenic pollution because of direct deposition by runoff water from roads, industrials wastes and agriculture waste.

The most commonly employed methods for removing mercury and arsenic are chemical or electrochemical precipitation, both of which pose a challenge in terms of disposal of the precipitated wastes, and ion-exchange treatments, which are not economical [13, 14]. Consequently, a robust, ecofriendly, and economical removal methods are essential. In this work, fish scales waste remains, that are readily and cheaply available has been employed as an ecofriendly and economical alternative for removing mercury and arsenic from wastewater effluent. The adsorption nature of the fish scale waste remains (FSWR) was intensively investigated. Standard Langmuir and Freundlich and Dubinin-Radushkevich models were applied to the experimental data to evaluate the adsorption isotherm of the FSWR. The adsorption kinetics and thermodynamics were also investigated. The effects of initial concentration, pH, contact time, and FSWR dosage on the adsorption process of the FSWR were studied as well.

2. Materials and Instrumentations

The adsorbents used for the experiments were fish scales collected from fishes from water bodies around Palapye, Botswana. Ultra-pure water of 18.0 MΩ/cm resistivity, Type I, was prepared by a Elix 5 Millipore water purification system from Merck, (Darmstadt, Germany) and was used to prepare all solutions. Reagents used were: analytical grade HCl (37%) purchased from ACE (Johannesburg, South Africa). SPAR white spirit Vinegar, which was employed to treat the waste materials, was purchased from SPAR (Palapye, Botswana). Elemental standard solutions used [1000ppm – Hg (II) and As (III)] and NaOH (97%) pellets were purchased from Rochelle Chemicals (Johannesburg, South Africa). A Mars6 One Touch Microwave Assisted Extractor/Digester (CEM Microwave Technology Ltd, North Carolina, USA) obtained from CEM (Johannesburg, South Africa) was employed to digestion and extraction of heavy metals from the fish scales. For determination of size, morphology and nanoparticle composition, JSM 1700 SEM coupled with EDX, obtained from (JOEL, USA) was employed. Perkin Elmer System, Spectrum two Fourier transform infrared (FTIR) spectroscopy was employed to determine the functional groups of the fish scales. A powder D8 Advanced Powder X-Ray Diffractometer (XRD) obtained from Bruker (Karlsruhe, Germany) was employed for characterization of the fish scales. Heavy metals were determined by an iCAP 7000 series Thermo Scientific inductively coupled plasma spectrometer (ICP – OES), (Johannesburg, South Africa).

3. Pre-treatment of the Fish Scales Waste Remains

The fish scales waste remains were obtained from fishes collected from water bodies around Palapye, Botswana. They were washed systematically with deionized water to remove mud and other impurities. After which, they were sun dried for two days and pulverized employing a Fritsch pulverisette 5 pulverizer obtained from Fritsch (Berlin, Germany), operated at 400 rpm for 90 min in both milling and reverse mode. The pulverized materials were sieved employing 63 – 200 micron mesh size. After screening they were again washed with deionized water several times to remove persistent impurities. The material was than treated with SPAR white spirit vinegar to remove inorganic pollutants. Finally, they were dried in an oven at 65 ± 5°C for 6 hrs [15].

4. Characterization of Treated FSWR

4.1. Fourier Transform Infrared Spectroscopy (FT-IR)

Fourier transform infrared (FTIR) spectrometer was employed to investigate the functional groups responsible for

the heavy metals uptake and bonding that exists on the surface of the fish scales. The FTIR spectra were recorded in the wavelength range 500 - 4000 cm^{-1} on a Nicolet iS10 Thermo Scientific FTIR. The data were collected at 2.0 cm^{-1} resolution, with each spectrum the result of 256 scans.

4.2. X-ray Powder Diffraction (XRD)

A powder D8 Advanced Powder X-Ray Diffractometer (XRD) analysis was employed to further investigate the physical properties, specifically the crystallinity of the waste material and the treatment effect. The XRD was operated with Cu Kα emission (ƛ = 1.54105Å, 40 kV, 40 mA per sec) with high efficiency linear detector of Lynx Eye type. The scanning mode employed was coupled with 2Θ/Θ on the scanning range 10˚ - 120˚ values. Deby-Scherrer method was employed to calculate the crystallite size of the pulverized FSWR.

4.3. Scanning Electron Microscopy Coupled with Energy Dispersive X-ray Spectroscopy (SEM-EDX)

Scanning Electron Microscope coupled with Energy-dispersive X-ray spectroscopy (SEM - EDX) (JSM – 7100F), was employed to determine the surface morphology of the pulverized FSWR and also to determine its elemental composition. E6700 Polaron range high vacuum pressure sputter coater (Quorum Technologies, UK) was employed for carbon coating of the FSWR. The coated material was taken for SEM-EDX analysis, which operated under high vacuum and beam acceleration voltage of 10.0 kV (the recommended operating voltage for organic material samples).

5. Batch Adsorption Studies for Hg (II) and As (III) Employing FSWR

All experiments were carried out in batches and done in triplicates. A 100 mg/L standard mixture of Hg (II) and As (III) was prepared from 1000 ppm stock solution of each of the cations. The FSWR employed were of particle size of ≤ 63 µm.

5.1. Optimization of Factors Affecting Adsorption of Hg (II) and As (III)

A multivariate optimization methodology was employed to model the optimization of factors affecting the adsorption of Hg (II) and As (III) by the FSWR. In this study, the effect of four factors, namely contact time, pH, FSWR dosage, as well as initial Hg (II) and As (III) concentration were investigated. Firstly, a two-level fractional factorial design employed to enable identification of the significance of each factor towards the experimental output. Following this, a face centered central composite design was then performed to determine the optimum conditions for each factor that would result in a maximized response of the experiments. The optimization process was carried out with the use of Minitab Release 14 statistical software (Minitab Inc., USA).

The low and high levels of each factor were established considering previous experiments from literature. It was then filtered into a 250 mL volumetric flask and deionized water added to the mark. It was investigated for cations employing inductively coupled plasma optical emission spectrometer (ICP-OES).

Table 1. Factors and their levels for the two-level fractional factorial design for the optimization of the FSWR.

Variable	Factor	Low level	High level
A	FSWR dosage (mg)	10	1000
B	pH	2	10
C	Contact time (minutes)	5	180
D	Concentration (mg/L)	0	50

The significant factors from the screening phase (two-level ½ fraction factorial design) were all used for the optimization phase (CCD). The experiments were done in triplicate. It was then filtered into a 250 mL volumetric flask and deionized water added to the mark and investigated for cations employing ICP-OES.

5.2. Determination of Hg (II) and As (III) within Wastewater Sample

50 mL of the wastewater sample was measured and added to an aqua regia solution of HCl: HNO_3 at a ratio of 3:1 v/v. The mixture was transferred to a 100 mL TFM sample vessel and then digested employing a MARS6 microwave assisted digester operated at a pressure of 600 psi, temperature of 100°C and 1200 W. The ramp time was set at 20.0 min with a hold time of 10.0 min. The resulting volume was transferred to a 50 mL volumetric flasks. Deionized water was added to the flasks and filled up to the mark. The samples were investigated for Hg (II) and As (III) employing ICP-OES.

5.3. Application of Optimized Adsorption Method to Wastewater Sample

The removal efficiency of Hg (II) and As (III) by the FSWR was investigated by applying the optimized adsorption method to wastewater samples collected from sewage treatment plant. The mixture was subjected to a rotary shaker at 200 rpm for the optimized time, after which it was then filtered using a Whatman No. 1 filter paper and put into 50 mL volumetric flasks. Deionized water was added to the flasks and filled up to the mark.

The analysis was done in triplicates, and Hg (II) and As (III) standards (from 5 ppm to 50 ppm) were prepared for the calibration curve. The effluent was then investigated by employing ICP – OES. The percentage removal of chloride and fluoride anions was calculated using the formula below

$$\frac{Ci-Cf}{Ci} \times 100 \quad (1)$$

Where

Ci is the initial concentration of metal ions in wastewater sample.

Cf is the final concentration of metal ion in wastewater after applying the eggshell waste remains.

The results analysed using Microsoft Excel 2016.

5.4. Adsorption Isotherm

Adsorption equilibrium studies were conducted to study the kind of the adsorption isotherms and the adsorption capacity of the FSWR for the removal of Hg (II) and As (III). For the isotherm studies, the initial ions concentrations were varied from 10 to 100 mg/L using 1 g/L (dry weight) FSWR powder. The mixture was batched in a rotary shaker at 400rpm and samples were collected at specified time intervals, and then filtered. The effluent was investigated employing ICP OES

During adsorption, a rapid equilibrium is established between Hg (II) and As (III) and the FSWR [16]. The equilibrium ion uptake q is calculated using the following equation:

$$q = \frac{(Ci-Cf)V}{M} \quad (2)$$

Where, *V* is the volume of the solution, C_i and C_f are initial and equilibrium concentrations and M is the dry mass of FSWR [13]. The Langmuir equation which is only effective for monolayer sorption on to a surface with a finite number of identical sites is given by equation:

$$q = \frac{qmax\ bCf}{1+bCf} \quad (3)$$

Where q_{max} is the maximum amount of the Hg (II) and As (III) ions per unit weight of the FSWR to form a complete single layer on the surface bound at high C_f. *b* is a constant related to the affinity of the binding sites q_{max} and it represents an applied limiting adsorption capacity when the FSWR surface is fully covered with Hg (II) and As (III) ions. It also assists in the comparison of adsorption performance mostly in an event where the sorbent did not reach its full saturation in experiments [17]. q_{max} and *b* can be determined from the linear plot of C_f/q versus C_f [18]. The linearized form of this model equation is given as:

$$\frac{Cf}{q} = \frac{Cf}{qmax} + \frac{1}{bqmax} \quad (4)$$

The empirical Freundlich model indicates that the adsorbent (FSWR) has a heterogeneous surface so that binding sites are not identical [18]. This model takes the following form for a single component adsorption.

$$q = KCf^{A/n} \quad (5)$$

Where *K* and *n* are the Freundlich constants characteristic of the system. *K* and *n* are indicators of adsorption capacity and adsorption intensity respectively [19]. The Freundlich isotherm provides no information on the monolayer adsorption capacity, in contrast to the Langmuir model

$$Logq = logK + 1/n\ logCf \quad (6)$$

Langmuir and Freundlich isotherms are usually accompany by additional models to explain the physical and chemical characteristics of adsorption. For instance, Langmuir isotherm constants cannot explain the chemical or physical properties of the adsorption process. However, the mean adsorption energy (E) calculated from the D-R isotherm provides important information about these properties. Dubinin – Radushkevich (D-R) isotherm is commonly used to describe the adsorption isotherms of single solute systems [20]. The D-R isotherm is expressed as:

$$q = q_{max}\ exp$$

$$q = q_{max}\ \exp[-B[RT\ In[1 + \tfrac{1}{Cf}]]^2] \quad (7)$$

$$In\ q = In\ qmax - Be^2 \quad (8)$$

Where *B* is a constant related to the adsorption energy, *R* is the gas constant (8.314x10-3kJ/molK) and *T* is the absolute temperature

$$e = RT\ In\ [1 + \tfrac{1}{Cf}] \quad (9)$$

$$E = \frac{1}{(2B)^{0.5}} \quad (10)$$

This equation gives information about the physical and chemical adsorption. With the magnitude of *E* between 8 and 16 kJmol^{-1} the adsorption process follows chemical ion exchange, while for the values of $E < 8$ kJmol^{-1}, the adsorption process is of a physical nature [18].

5.5. Kinetic Studies

Kinetic studies were carried out at different intervals of 5 min to 180 min. The effluents were analysed for residual Hg (II) and As (III) ions concentration.

Three kinetic models, pseudo first order, second order and intra particle diffusion models were employed to investigate the kinetics of adsorption. First order rate equation was

applied to the experimental adsorption data,

$$\frac{dq}{dt} = k_1\,(qe - q) \tag{11}$$

Where q_e and q are the adsorption capacity at equilibrium and at time t respectively, and k_1 is the rate constant of the pseudo first order adsorption process [21]. The integrated linear form of Eqn. (11) can be expressed as follows:

$$\log(qe - q) = \log(qe) - \frac{k_1}{2.303}t \tag{12}$$

Plot of *log* $(q_e\text{-}q)$ vs. t gives a straight line for first order adsorption kinetics and the rate constant k_1 is computed from the plot. The sorption data was also studied by second order kinetics [22],

$$\frac{dq}{dt} = k_2(qe - q)^2 \tag{13}$$

Where k_2 is the second order rate constant.

After integration,

$$\frac{1}{qe-q} = \frac{1}{qe} + k_2 t \tag{14}$$

This can be written in the linear form on further simplification

$$\frac{t}{q} = \frac{1}{k_2 qe^2} + \frac{t}{qe} \tag{15}$$

The applicability of this equation can be studied by a plot of t/q. Intra particle diffusion was characterized using the relationship between specific sorption (q) and the square root of time ($t^{1/2}$) [23]. The relation is expressed as follows:

$$q = k_d t^{1/2} \tag{16}$$

5.6. Thermodynamic studies

Thermodynamic studies were conducted at different temperatures in the range of 0 – 50°C in a rotary shaker for 90 min. The samples were filtered and analysed employing ICP OES for the residual Hg (II) and As (III) concentrations at the end of the experiments.

Reaction occurs spontaneously at a given temperature if ΔG is a negative quantity [24]. The free energy of the sorption reaction considering the sorption equilibrium constant is given by the following equation:

$$\Delta G = -RTlnb \tag{17}$$

Where ΔG is the changes in Gibbs free energy, R (8.314 J/mol K) is the universal gas constant, T (K) the absolute temperature and b (L/mol) the thermodynamic equilibrium constant. Considering the relationship between free energy and the equilibrium constant, change in equilibrium constant can be obtained in the differential form as follows [25]:

$$\frac{dlnb}{dT} = \frac{\Delta H}{RT^2} \tag{18}$$

After integration,

$$lnb = -\frac{\Delta H}{RT} + Y \tag{19}$$

Where Y is a constant, the above equation can be rearranged to obtain

$$-RT\,lnb = \Delta H - TRY \tag{20}$$

$$\text{Let } \Delta S = RY \tag{21}$$

Substituting equations (17) and (21) into (20), the Gibbs free energy change, ΔG, can be represented as follows.

$$\Delta G = \Delta H - T\Delta S \tag{22}$$

A plot of Gibbs free energy (ΔG) versus temperature T was found to be linear. The values of enthalpy change ΔH and entropy change ΔS were determined from the slope and intercept of the plots [23].

6. Results and Discussions

6.1. FT-IR

To characterize the FSWR for the presence of functional groups responsible for Hg (II) and As (III) interaction with the FSWR, fourier transform infrared spectrometer (FTIR) was employed. The functional groups of fish scales before removal (black) and after removal (red) of target analytes are shown in Figure 1. The prominent functional groups in the fish scales are 1016 cm^{-1} due to carboxyl bands and primary amines, 554 to 597 cm^{-1} due to alkanes, 870 cm^{-1} due to sulphonates, -OH and N-H groups at 3286 cm^{-1}, C-O group at 1542.1 to 1642.4 cm^{-1} and C-H, $-CH_3$, $-CH_2$ groups at 1408.4 cm^{-1}

Hg (II) and As (III) interacted with different functional groups leading to the decrease of intensities and shift of the mentioned peaks as shown in Figure 1. These interactions may perhaps be the result of complex formation of Hg (II) and As (III) with the FSWR surface functional groups. Usually, complexation of metal ions with functional groups is responsible for the removal of metal from the water samples. Heavy metals forms coordinate bonds with the different functional groups and hence cause a decrease in peak intensity and also shift in peaks. Functional groups such as amines, carboxylic, hydroxyl, carbonyls form anionic sites as pH is raised from acidic to basic conditions. The negatively charged sites are responsible for binding with the heavy metals.

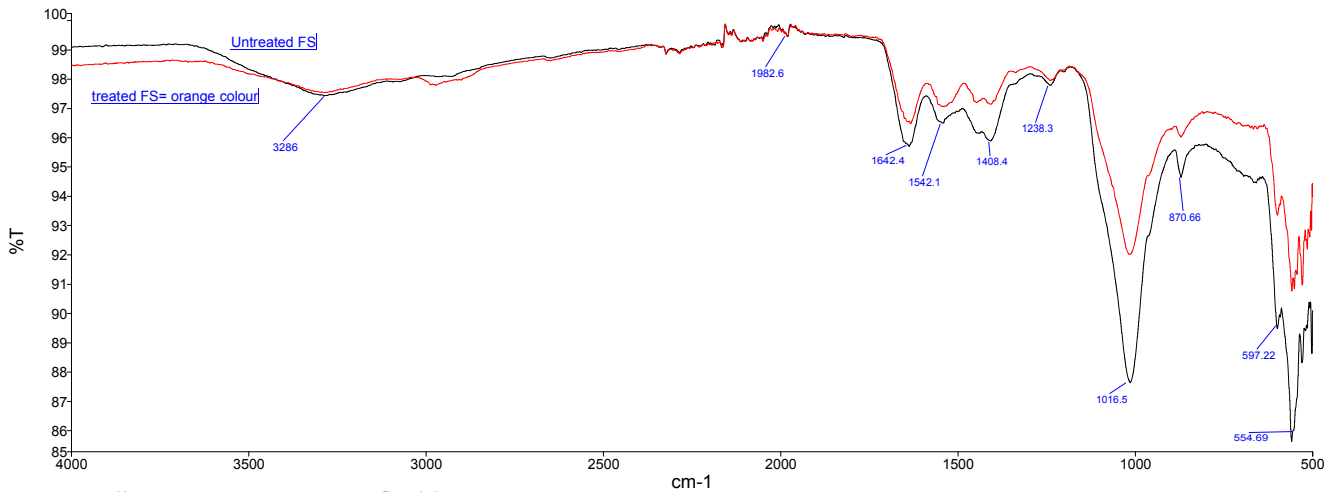

Figure 1. FTIR of FSWR before removal (black) and after removal (red) of Hg (II) and As (III).

6.2. X-ray Powder Diffraction (XRD)

The XRD phase analysis of the fish scales were performed using JCPDS (Joint Committee on Powder Diffraction Standards) card number 01-073-0293 that showed a compound of *hydroxyapatite* with a chemical formula $Ca_5(PO_4)_3(OH)$, $Ca_{10}(PO_4)_6(OH)_2$, and $Ca_{10}(PO_4)_6(OH)_2$ for the treated fish scales (TFs) powder, the untreated fish scales (UFs) powder and the fish scales powder after adsorption AFs) respectively (see Figure 2). The powder X-ray diffraction patterns of the fish scales (TFs, UFs and AFs) showed increasing intensity of the reflections in the order of AFs > UFs > TFs, with *d-spacings* of 0·735, 0·564, 0·534, 0·466, 0·401, 0·342, 0·243, and 0·182 for AFs; 0·561, 0·511, 0·457, 0·401, 0·335 and 0·297 for UFs and 0·242 and 0·189 for TFs corresponding to the hydroxyapatite structure [26, 27].

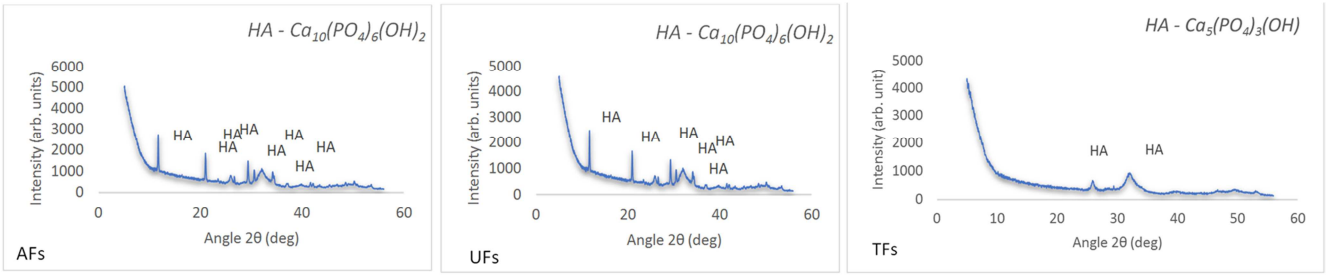

Figure 2. XRD diffractogram of the AFs, UFs and TFs powders.

6.3. SEM – EDX

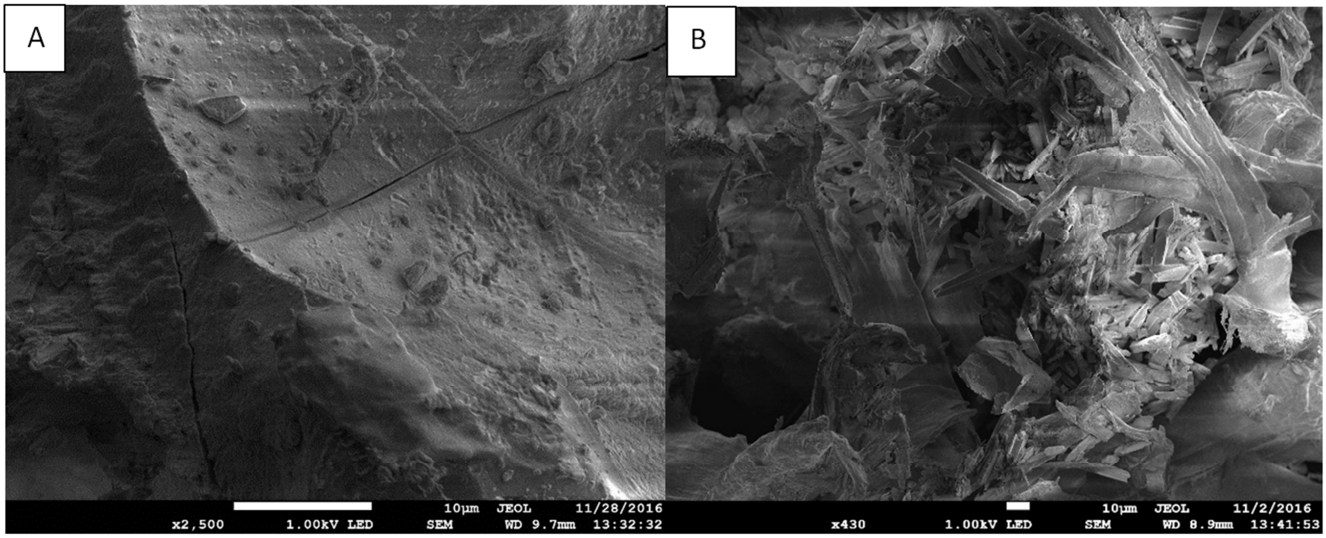

Figure 3. SEM images of the A) TFs and B) AFs powders.

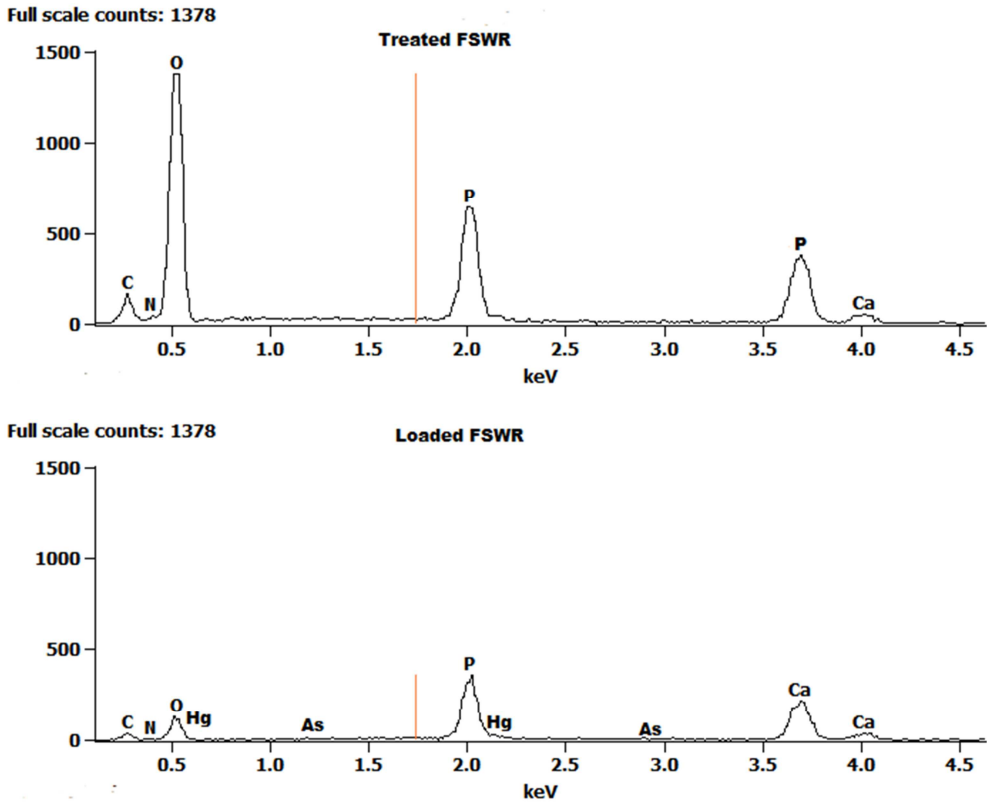

Figure 4. EDX of the treated FSWR and the loaded FSWR.

Figure 3 shows SEM micrographs of the FSWR. The fish scale seems to have a rough surface with a particle size of ≤63 µm and are characterized by having two regions; a darker and a white region. The white region is rich in inorganic material containing high proportion of calcium and phosphorus whereas the dark region is rich in protein because it has high proportion of carbon and oxygen. From energy dispersive X-ray (EDX) analysis, inorganic ions were confirmed in the fish scales before treatment and after adsorption as shown in Figure 4. This micrograph clearly shows that the presence of new shiny bulky particles over the surface of ions loaded fish scale (AFs) which are absent in the TFs [28]. These results confirm the binding of Hg (II) and As (III) onto the FSWR via adsorption.

6.4. Determination of Hg (II) and As (III) within the Wastewater Sample

Underground waters from local boreholes is the main water source for local people in Botswana, however, most of the boreholes have low capacity [29]. The supply does not meet the demands for irrigation. Irrigation schemes using the wastewater have been set up round the Glen Valley wastewater treatment plant, in Gaborone [30]. Because of these factors, wastewater sample were ideal to be used as the real water samples in this work. The initial total As (III) and Hg (II) concentrations from the digested wastewater samples were determined as 0.142 ± 0.0034 and 0.007 ± 0.0002 mg/L respectively

As (III) and Hg (II) concentrations in all the sampling points in the wastewater treatment plant were found to be within the allowed levels set by waste water specification-BOS 93:2012 in Botswana and US EPA [31]. As the result of the low concentrations of the selected ions, the sample was spiked with 2 mg/L of each of the selected metal ions.

6.5. Optimization of Factors Affecting Adsorption of Hg (II) and As (III)

Experimental matrices were designed using Minitab for the optimization purposes. The yields were followed by the use of ICP OES separation measurements of Hg (II) and As (III). Prior to performing the actual optimization, a ½ fraction factorial design was employed in order to assess the level of significance of each factor under investigation. The factorial design comes as a screening phase, which allows screening a relatively large number of factors in a relatively small number of experiments that cover the whole experimental domain, with the result identifying the most influential factors towards obtained yields. Analysis of data was in the forms of normal probability plots of standardized effects, and residuals plots; as shown by Figures 5 and 6, respectively.

From the normal probability plot of standardized effects, the magnitude of the main effects of each factor as well as the effects brought about by the interaction of factors, towards

the obtained yield are investigated. The magnitude of each type of effect is represented by its distance from the solid line, as well as the side on which the effect lies with respect to the solid line. Negative effects lie to the left while positive effects lie to the right of the solid line. The solid line indicates where the points would drop if the effects were zero, while the percentage in the y-axis signifies the weightage of each factor's contribution towards the obtained yield. The investigated effects exhibited a positive magnitude as they all appeared to the right of the graph, as can be observed in Figures 5. The main effects, due to Factors A (Contact time), B (pH), C (FSWR dosage) and D (initial concentration) were significant for the selected metal ions. Factor D for both anions lay furthest to the right of the solid line, signifying that factor D had a greater positive magnitude towards contribution of the yields obtained. However, the contribution of each factors (A, B, C, and D) showed higher weightage towards the output as compared to that of effects brought about by the interaction of factors.

Figure 6 shows the residual plots for the yield obtained when using the FSWR powders. The plots explain the distribution pattern of data points through the use of residuals. Residuals are the outcome of the difference between the observed and the fitted values [32]. Normal probability and histogram plots investigate whether the data obtained exhibits a standard Gaussian distribution. For normal probability plots, if the data points fall approximately along the straight line, then the residuals are said to be normally distributed, meaning the data follows the Gaussian distribution [33], which was the case for this work. A plot of residuals against fitted responses (values) is used to detect unequal error variances and outliers, while the plot of residuals against order of the data checks for correlation of the residuals. The residuals against fitted values plot revealed a constant variance of the residuals about the center line. The plot of residuals against order of the data showed a randomized shifting pattern about the center line, signifying that the data was uncorrelated with each other. The plots for the FSWR show that the residuals were randomly distributed, hence, signifying absence of systematic errors and hence adequacy of the model.

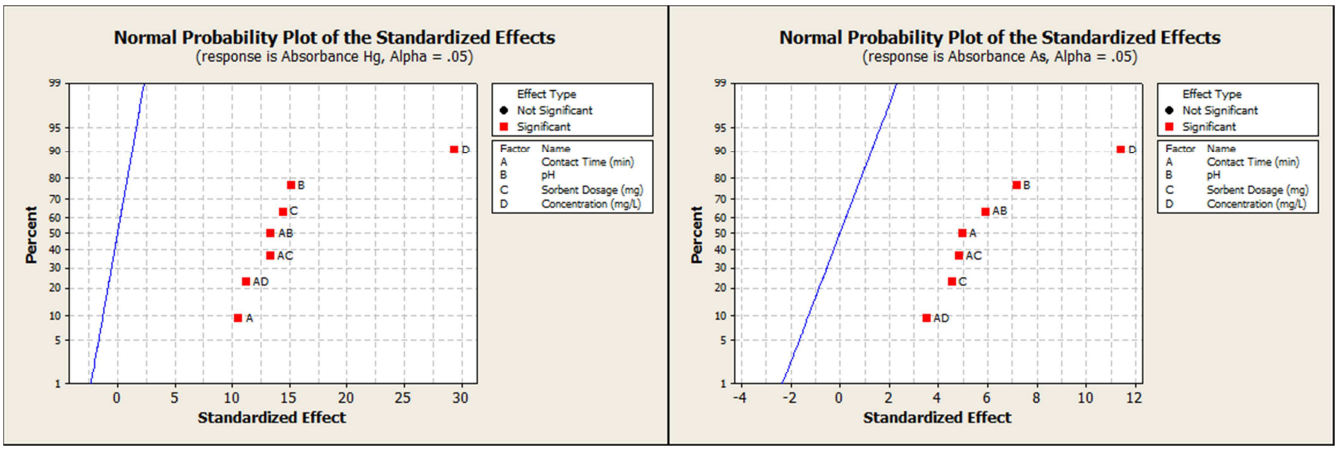

Figure 5. The normal probability plots of standardized effects of Hg (II) and As (III) for the FSWR.

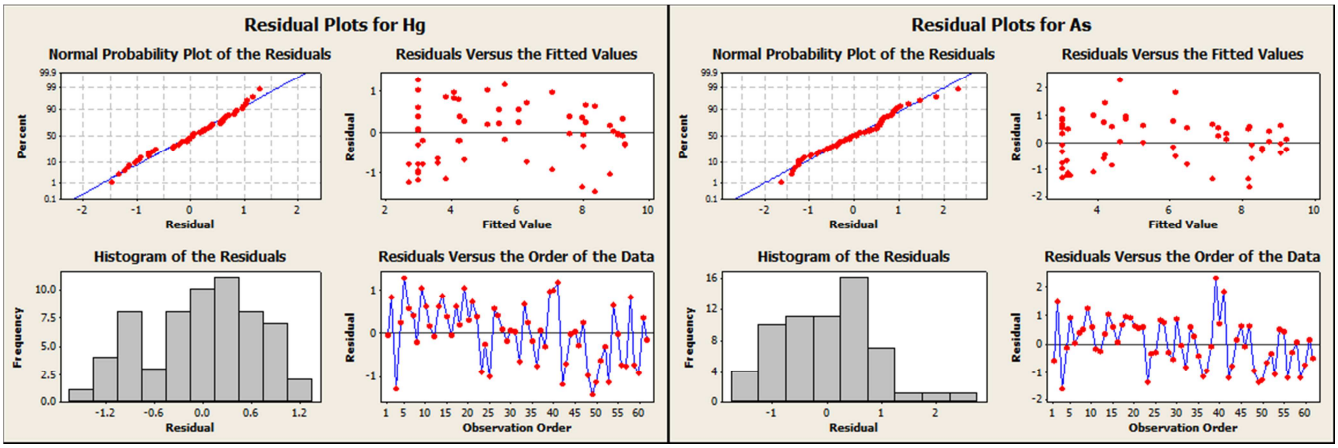

Figure 6. Residuals plots of standardized effects on the FSWR.

Following the screening of significant factors using fractional factorial design, a response surface design was then created to determine the optimum conditions of each factor. This was achieved through the use of a CCD. The optimal conditions

obtained for the FSWR adsorption of Hg (II) and As (III) were 22.63 and 23.85 mg/L for the initial ions concentration respectively, the sorbents dose was found to be 76.99 mg/L [Hg (II)] and 78.82 mg/L [As(III)], contact time, were found to be 74.84 min [Hg (II)] and 63.89 min [As(III)] and solution pH 7.29 [Hg (II)] and 7.78 [As(III)]. Furthermore, the regression coefficient, R^2, was also used to assess the fit of the model to the experimental data for Hg (II) and As (III) which were 0.9789 and 0.9910 respectively. The relative standard deviations (RSD) for the experimental data were obtained to be 2.06% and 1.66% for Hg (II) and As (III) respectively.

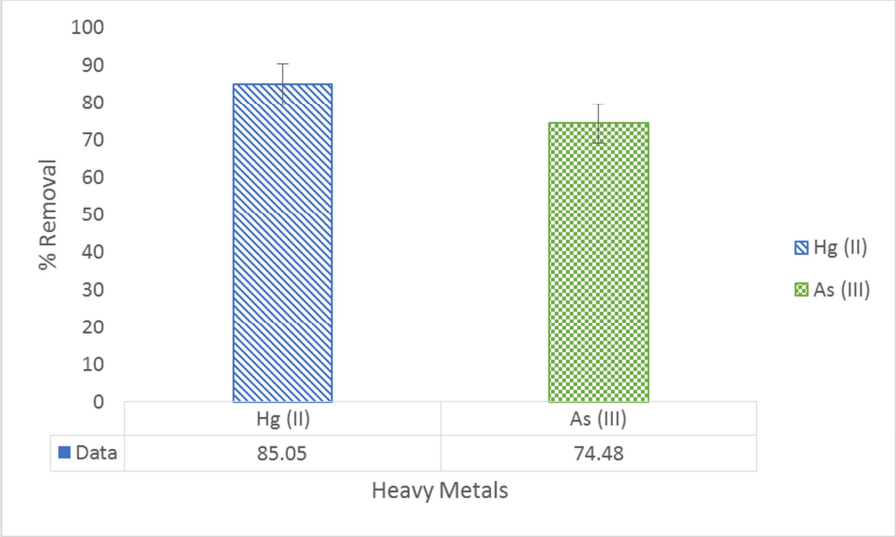

Figure 7. Percentage removal of Hg (II) and As (III) from wastewater sample employing the FSWR.

6.6. Application of Optimized Adsorption Method to Wastewater Sample

After evaluation of the factors affecting adsorption, the parameters were applied in a 50 mL of the wastewater sample and the resulting effluent was analysed employing ICP-OES. Figure 7 above represent the percentage removal of Hg (II) ion (85.05% ± 1.69%) and As (III) ion (74.48% ± 1.09%) from real wastewater samples. The FSWR showed excellent removal efficiency towards the selected cations. The recoveries of spiked ions were 101% and 105% for Hg (II) and As (III) respectively.

6.7. Adsorption Isotherm

In view of the values of the linear regression coefficients, Langmuir model fits very well to the sorption data in the studied concentration range studied. According to the Table 2, the affinity order of the FSWR is As > Hg. The higher the b, the higher is the affinity of the adsorbent for ions. q_{max} can also be interpreted as the total number of binding sites that are available for adsorption and q_e as the number of binding sites that are in fact occupied by the ions at the concentration C_e [34]. The adsorption energies are less than 2 $kJmol^{-1}$ suggesting that the sorption process was dominated by physical forces at all studied temperatures.

Table 2. Equilibrium studies parameters for the FSWR.

Ions	Temp. (K)	Langmuir Model			Freundlich Model			Dubinin – Radushkevich Model		
		R^2	$q_{max\ (mg/g)}$	b (L/mg)	R^2	K	1/n	R^2	E (J/mol)	$q_{max\ (mg/g)}$
Hg	298.15	0.9711	34.48	0.13	0.626	0.43	1.02	0.9012	320.35	15.75
	308.15	0.994	48.31	0.05	0.8454	0.68	1.09	0.9705	469.35	15.15
	318.15	0.9831	30.21	0.07	0.8933	0.82	1.02	0.98	592.81	15.17
	333.15	0.9894	34.03	0.01	0.9465	1.30	1.09	0.9823	952.45	15.18
As	298.15	0.9528	28.82	0.15	0.6468	0.46	1.01	0.966	337.12	15.98
	308.15	0.9717	27.70	0.09	0.8447	0.72	1.03	0.9756	499.02	15.42
	318.15	0.9983	32.46	0.02	0.9848	1.28	1.18	0.9801	717.88	15.38
	333.15	0.9955	22.32	0.04	0.9948	1.46	1.14	0.9798	900.97	15.36

6.8. Adsorption Kinetics

The comparison of experimental sorption capacities (q_{exp}) and the predicted values (q_{cal}, k_1, k_2, k_d, R2) from pseudo first order, pseudo second order and intra particle diffusion constants are given in Table 3 for the FSWR. The pseudo first order was not satisfactory to explain the experimental data, whereas the calculated, q_{cal} values derived from the pseudo second order model for sorption of the selected ions were very close to the experimental (q_{exp}) values. The second order equation appeared to be the better fitting model than first order and intra particle diffusion equations because it has higher R^2 value [21, 35].

Table 3. Adsorption kinetic parameters of the FSWR.

Ions	q_{exp} (mg/g)	Second Order			First Order			Intra Particle Diffusion	
		R^2	K_2 ($gmg^{-1}min^{-1}$)	q_{cal} (mg/g)	R^2	K_1 (min^{-1})	q_{cal} (mg/g)	R^2	K_d ($mgL^{-1}min^{-1/2}$)
Hg	11.43	0.9777	0.017	12.01	0.7446	0.030	0.32	0.5305	0.220
As	11.33	0.9983	0.027	12.73	0.9209	0.023	0.16	0.5758	0.234

6.9. Adsorption Thermodynamics

The negative values for the Gibbs free energy for Hg (II) and As (III) ions as shown in Table 4 show that the adsorption process is spontaneous and that the degree of spontaneity of the reaction increases with increasing temperature. The overall adsorption process seems to be endothermic [ΔH = 43.96 and 54.18 $kJmol^{-1}$ for Hg (II) and As (III) respectively]. The ΔS values were positive, implying that entropy increases as a result of adsorption. This may have occurred as a result of redistribution of energy between the Hg (II) and As (III) ions and the FSWR. Before adsorption occurs, the Hg (II) and As (III) ions near the surface of the FSWR will be more ordered than in the subsequent adsorbed state and the ratio of free ions to ions interacting with the adsorbent will be higher than in the adsorbent state. As a result, the distribution of rotational and translational energy among a small number of metal ions increase with increasing adsorption by producing a positive value of ΔS and randomness will increase at the solid solution interface during the process of adsorption. Thus, adsorption is likely to occur spontaneously at normal and high temperatures if $\Delta H>0$ and $\Delta S>0$.

Table *4*. Thermodynamic parameters for the adsorption of Hg (II) and As (III) ions onto the FSWR.

Ions	Temp. (K)	b (L/mol)	ΔG (kJ/mol)	ΔH (kJ/mol)	ΔS (kJ/molK)	R^2
Hg	298.15	18607.60	-24.37	43.96	0.3678	0.9832
	308.15	34668.20	-26.78			
	318.15	66907.90	-29.39			
	333.15	119898.00	-32.39			
As	298.15	6126.08	-21.62	54.18	0.4481	0.9896
	308.15	14924.70	-24.62			
	318.15	32717.00	-27.50			
	333.15	60862.70	-30.51			

7. Conclusion

This study showed that fish scales waste remains which are widely available at low cost can be used as an efficient biomaterial for the removal of Hg (II) and As (III) from wastewater. IR spectrum analysis showed different functional groups present in the FSWR including OH, CH stretching, C=C stretching, C-O stretching. The XRD diffractogram suggested the presence of hydroxyapatite in the valuarized fish scales. Initial Hg (II) and As (III) concentration, pH, contact time, FSWR dosage and its characteristics were the factors responsible for Hg (II) and As (III) ions adsorption. This study demonstrated that fish scales waste remains are environmental friendly, economical and readily available waste biomaterials with high efficacy for the removal of excess toxic heavy metal ions from wastewater as shown by Hg (II) and As (III) ions. Most significantly, this study has created an alternative method for agricultural and industrial waste management, particularly for fisheries and food industries. Additionally, the study achieved the phenomenon of valuarizing waste material which is essential in the today's industrial world.

Acknowledgements

This is to acknowledge the Department of Chemical and Forensic Sciences of Botswana International University of Science and Technology (BIUST) for fully funding this research through its postgraduate research funds (2015 – 2017).

Conflicts of Interest

All the authors do not have any possible conflicts of interest.

References

[1] S. K. Gunatilake, "Methods of Removing Heavy Metals from Industrial Wastewater," *J. Multidiscip. Eng. Sci. Stud.*, vol. 1, no. 1, pp. 12–18, 2015.

[2] L. M. Plum, L. Rink, and H. Haase, "The Essential Toxin: Impact of Zinc on Human Health," *Int. J. Environ. Res. Public Health*, vol. 7, no. 4, pp. 1342–1365, Mar. 2010.

[3] M. Karnib, A. Kabbani, H. Holail, and Z. Olama, "Heavy metals removal using activated carbon, silica and silica activated carbon composite," *Energy Procedia*, vol. 50, pp. 113–120, 2014.

[4] S. Vigneswaran and M. Sundaravadivel, "Recycle and reuse of domestic wastewater," *Encyclopedia of Life Support Systems (EOLSS)*. Encyclopedia of Life Support Systems (EOLSS), 2004.

[5] C.-Y. Chen, S.-N. Chang, and G.-S. Wang, "Determination of ten haloacetic acids in drinking water using high-performance and ultra-performance liquid chromatography-tandem mass spectrometry.," *J. Chromatogr. Sci.*, vol. 47, no. January, pp. 67–74, 2009.

[6] A. S. Alturiqi and L. a. Albedair, "Evaluation of some heavy metals in certain fish, meat and meat products in Saudi Arabian markets," *Egypt. J. Aquat. Res.*, vol. 38, no. 1, pp. 45–49, 2012.

[7] X. Lu, L. Y. Li, L. Wang, K. Lei, J. Huang, and Y. Zhai, "Contamination assessment of mercury and arsenic in roadway dust from Baoji, China," *Atmos. Environ.*, vol. 43, no. 15, pp. 2489–2496, 2009.

[8] B. K. Asare and M. B. K. Darkoh, "Socio-Economic and Environmental Impacts of Mining in Botswana: A Case Study of the Selebi-Phikwe Copper-Nickel Mine.," *East. Afr. Soc. Sci. Res. Rev.*, vol. 17, pp. 1–41, 2001.

[9] S. Banga and P. K. Varshney, "Effect of impurities on performance of biodiesel: A review," *J. Sci. Ind. Res. (India).*, vol. 69, no. 8, pp. 575–579, 2010.

[10] L. Allen, M. J. Cohen, D. Abelson, and B. Miller, "Fossil fuels and water quality," *The Worlds Water*, vol. 1994, no. 7, pp. 73–96, 2011.

[11] National Research Council, *Toxicological effects of methylmercury*. 2000.

[12] J. M. Campos-Martin, M. C. Capel-Sanchez, P. Perez-Presas, and J. L. G. Fierro, "Oxidative processes of desulfurization of liquid fuels," *J. Chem. Technol. Biotechnol.*, vol. 85, no. 7, pp. 879–890, 2010.

[13] M. a. Barakat, "New trends in removing heavy metals from industrial wastewater," *Arab. J. Chem.*, vol. 4, no. 4, pp. 361–377, 2011.

[14] M. E. Argun and S. Dursun, "Removal of heavy metal ions using chemically modified adsorbents," *J. Int. Environ. Appl. Sci*, vol. 1, no. 1–2, pp. 27–40, 2006.

[15] A. Bhatnagar and M. Sillanp, "Utilization of agro-industrial and municipal waste materials as potential adsorbents for water treatment-A review," *Chem. Eng. J.*, vol. 157, no. 2–3, pp. 277–296, 2010.

[16] G. Crini, "Non-conventional low-cost adsorbents for dye removal: A review," *Bioresour. Technol.*, vol. 97, no. 9, pp. 1061–1085, 2006.

[17] H. Ahmad Panahi, M. Samadi Zadeh, S. Tavangari, E. Moniri, and J. Ghassemi, "Nickel adsorption from environmental samples by ion imprinted aniline -formaldehyde polymer," *Iran. J. Chem. Chem. Eng.*, vol. 31, no. 3, pp. 35–44, 2012.

[18] S. M. Nomanbhay and K. Palanisamy, "Removal of heavy metal from industrial wastewater using chitosan coated oil palm shell charcoal," *Electron. J. Biotechnol.*, vol. 8, no. 1, pp. 43–53, 2005.

[19] V. C. Renge, S. V Khedkar, and S. V Pande, "Removal of Heavy Metals From Wastewater Using Low Cost Adsorbents : a Review," *Sci. Revs. Chem. Commun*, vol. 2, no. 4, pp. 580–584, 2012.

[20] H. Li, W. Xu, N. Wang, X. Ma, D. Niu, B. Jiang, L. Liu, W. Huang, W. Yang, and Z. Zhou, "Synthesis of magnetic molecularly imprinted polymer particles for selective adsorption and separation of dibenzothiophene," *Microchim. Acta*, vol. 179, no. 1–2, pp. 123–130, 2012.

[21] N. Abd. Hadi, N. A. Rohaizar, and W. C. Sien, "Removal of Cu (II) from Water by Adsorption on Papaya Seed," *Asian Trans. Eng.*, vol. 1, no. 05, pp. 49–55, 2011.

[22] G. Bayramoglu and M. Y. Arica, "Synthesis of Cr(VI)-imprinted poly(4-vinyl pyridine-co-hydroxyethyl methacrylate) particles: Its adsorption propensity to Cr(VI)," *J. Hazard. Mater.*, vol. 187, pp. 213–221, 2011.

[23] M. Bhaumik, R. I. McCrindle, A. Maity, S. Agarwal, and V. K. Gupta, "Polyaniline nanofibers as highly effective re-usable adsorbent for removal of reactive black 5 from aqueous solutions," *J. Colloid Interface Sci.*, vol. 466, pp. 442–451, 2016.

[24] M. Przybyłek and J. Gaca, "Reaction of aniline with ammonium persulphate and concentrated hydrochloric acid: Experimental and DFT studies," *Chem. Pap.*, vol. 66, no. 7, pp. 699–708, 2012.

[25] C. Esen, M. Andac, N. Bereli, R. Say, E. Henden, and A. Denizli, "Highly selective ion-imprinted particles for solid-phase extraction of Pb^{2+} ions," *Mater. Sci. Eng. C*, vol. 29, pp. 2464–2470, 2009.

[26] S. Kumari and P. K. Rath, "Extraction and Characterization of Chitin and Chitosan from (Labeo rohit) Fish Scales," *Procedia Mater. Sci.*, vol. 6, no. Icmpc, pp. 482–489, 2014.

[27] N. Teramoto, A. Hayashi, K. Yamanaka, A. Sakiyama, A. Nakano, and M. Shibata, "Preparation and mechanical properties of photo-crosslinked fish gelatin/imogolite nanofiber composite hydrogel," *Materials (Basel).*, vol. 5, no. 12, pp. 2573–2585, 2012.

[28] K. Prabu, S. Shankarlal, and E. Natarajan, "A Biosorption of Heavy Metal Ions from Aqueous Solutions Using Fish Scale (Catla catla)," *World J. Fish Mar. Sci.*, vol. 4, no. 1, pp. 73–77, 2012.

[29] I. W. Maina, V. Obuseng, and F. Nareetsile, "Use of Moringa oleifera (moringa) seed pods and Sclerocarya birrea (morula) nut shells for removal of heavy metals from wastewater and borehole water," *Hindawi J. Chem.*, vol. 2016, pp. 1–33, 2016.

[30] V. Emongor, E. Nkegbe, B. Kealotswe, and I. Koorapetse, "Pollution Indicators in Gaborone Industrial effluent," *J. Appl. Sci.*, vol. 5 (1), no. ISSN 1607-8926, pp. 147–150, 2005.

[31] U S Environmental Protection Agency, *Environmental protection agency act, 1992*, no. 7. U S A, 1992, pp. 1–173.

[32] T. P. Ryan, "Modern Experimental Design," *Mod. Exp. Des.*, vol. 8608, no. April, pp. 1–601, 2006.

[33] E. R. Ziegel, *Statistics and Chemometrics for Analytical Chemistry*, vol. 46, no. 4. 2004.

[34] R. J. Umpleby, S. C. Baxter, M. Bode, J. K. Berch, R. N. Shah, and K. D. Shimizu, "Application of the Freundlich adsorption isotherm in the characterization of molecularly imprinted polymers," in *Analytica Chimica Acta*, 2001, vol. 435, pp. 35–42.

[35] M. Ikram, A. U. Rehman, S. Ali, S. Ali, S. Ul, and H. Bakhtiar, "The adsorptive potential of chicken egg shells for the removal of oxalic acid from wastewater," *J. Environ. Sci.*, vol. 2, no. 2, pp. 118–131, 2016.